Scientific Research Publishing

Advances in Materials Physics and Chemistry, 2024, 14, 15-23
https://www.scirp.org/journal/ampc
ISSN Online: 2162-5328
ISSN Print: 2162-531X

Structural, Magnetic and Heating Efficiency of Ball Milled γ-Fe_2O_3/Gd_2O_3 Nanocomposite for Magnetic Hyperthermia

Abdelaziz Sabik

Department of Physics, College of Sciences, Imam Mohammad Ibn Saud Islamic University (IMISU), Riyadh, Saudi Arabia
Email: amsabik@imamu.edu.sa

How to cite this paper: Sabik, A. (2024) Structural, Magnetic and Heating Efficiency of Ball Milled γ-Fe_2O_3/Gd_2O_3 Nanocomposite for Magnetic Hyperthermia. *Advances in Materials Physics and Chemistry*, **14**, 15-23.
https://doi.org/10.4236/ampc.2024.141002

Received: December 20, 2023
Accepted: January 23, 2024
Published: January 26, 2024

Abstract

The preparation of γ-Fe_2O_3/Gd_2O_3 nanocomposite for possible use in magnetic hyperthermia application was done by ball milling technique. The nanocomposite was characterized by X-ray diffraction (XRD) and vibrating sample magnetometer (VSM). The heating efficiency and the effect of milling time (5 h and 30 h) on the structural and magnetic properties of the nanocomposite were reported. XRD analysis confirms the formation of the nanocomposite, while magnetization measurements show that the milled sample present hysteresis with low coercivity and remanence. The specific absorption rate (SAR) under an alternating magnetic field is investigated as a function of the milling time. A mean heating efficiency of 68 W/g and 28.7 W/g are obtained for 5 h and 30 h milling times respectively at 332 kHz and 170 Oe. The results showed that the obtained nanocomposite for 5 h milling time is a promising candidate for magnetic hyperthermia due to his properties which show an interesting magnetic behavior and high specific absorption rate.

Keywords

Magnetic Hyperthermia, Iron Oxides Nanoparticles, Maghemite, Ball Milling, XRD, VSM

1. Introduction

Cancer is a disease, which is become one of the major public health concerns in the present world. Magnetic hyperthermia treatment is one of the promising non-invasive approaches for therapy on cancerous tumors upon exposure to external alternating magnetic fields (AMF). Magnetic nanoparticles (in the range of 10 to 100 nm) can generate heat through the oscillation of their magnetic

moments. Magnetic hyperthermia can then kill completely cancer cells by elevating their temperature between 42˚C and 46˚C with minimal injury to normal cells. This is an exciting potential therapy as it could replace or reduce the need for more destructive therapies such as chemotherapy [1] [2]. The most used materials for magnetic hyperthermia are ferrite nanoparticles in particular magnetite (Fe_3O_4) or maghemite (γ-Fe_2O_3). When exposed to an alternating magnetic field the magnetic nanoparticles produce heat via two main mechanisms, one is hysteresis loss and the other is relaxational loss (Neel and Brownian relaxations). The contribution of each process depends strongly on the nanoparticle size. For example, in small nanoparticles (20 nm), heat dissipation is due mainly to the Neel and Brownian relaxations with negligible contribution of hysteresis loss. For larger single-domain particles, hysteresis losses are significant.

In general, the heat generated per unit gram of magnetic material and per unit time under alternating magnetic field is known as specific absorption rate (SAR). Previous reports showed that the SAR values of the nanoparticles could be affected by several parameters such as sample preparation method, size of nanoparticles, magnetic properties, the amplitudes and frequency of the applied field, coating, etc. [3] [4] [5] [6] [7].

Most of the nanomaterials dedicated for magnetic hyperthermia are synthesized by chemical methods, due to the uniformity and the possibility to tune the size of nanoparticles. However, such methods use organic solvent and reducing agent in the synthesis process in addition to the difficulty to fabricate huge quantities. Others methods which are low-cost and friendly to the environment attracted an increasing interest during the last decades. Among these preparation methods, mechanical alloying is widely used to prepare nanocrystalline of a variety of materials as result of its simplicity, low cost and its capability to produce large volumes [8]. Lemine *et al.* [9] fabricated $Co_{1-x}Fe_xO_4$ Nanocrystalline for magnetic hyperthermia. They showed that the nanocrystalline dissipated heat under an AMF and this heat is able to kill cancerous cells. Ban *et al.* [10] used ball milled nickel-copper nanoalloys for magnetic hyperthermia. They investigated the effect of milling time for the optimization of the best sample, which gives the highest heating ability. Nanoalloys $Cu_{27.5}Ni_{72.5}$ (at%) alloy with a crystallite size of around 10 nm showed the best heating ability under an AMF.

The aim of this study is to prepare Gd_2O_3/γ-Fe_2O_3 nanocomposite by using ball milling technique for possible use in magnetic hyperthermia application. The effect of the milling time on the structure, morphology, magnetism and heating efficiency under an AMF of obtained nanocomposite will be investigated.

2. Materials and Methods

Commercially powders of Gd_2O_3 and maghemite (γ-Fe_2O_3) were introduced into a stainless-steel vial with balls in Fritsch machine (P7) for the preparation of $Gd_{0.05}Fe_{1.95}O_3$ nanocomposite. Two different milling times were considered (5 h and 30 h). The balls to powder ratio was fixed to 20:1. The rotation

speed was 300 rpm and the milling process was interrupted after every hour for ten minutes to prevent overheating. As-milled powder samples were characterized using X-ray diffraction (XRD) and vibratory sample magnetometry (VSM).

X-ray powder diffraction (XRD) measurements were performed using Bruker D8 Discover diffractometer (θ-2θ) equipped with Cu-Kα radiation (λ = 1.5406 Å). The average crystallite size, D, of all the samples was calculated from Scherer's equation [9] without considering the effect of lattice strains

$$D = \frac{K\lambda}{\beta \cos\theta} \tag{1}$$

where λ is the incident wavelength (1.5406 Å), θ is the Bragg angle (in degree), K is a constant whose value is approximately 0.9 and β (rad) is the full width at half maximum (FWHM) of a diffraction peak or integral breadth [11] [12].

The morphology was investigated through Field Scanning Electron Microscopy (FE-SEM, JEOL-6700F).

Magnetic measurements were measured at room temperature using Lake Shore 7404 model vibrating sample magnetometer (VSM) having a 1.8 T magnet. The magnetic parameters (*i.e.*, saturation magnetization (Ms), remanence magnetization (Mr), and coercivity (Hc)) were determined from the M-H curves.

The heating efficiency of the samples was carried out with a commercial system "Nanotherics Magnetherm" under alternating current (AC) magnetic field of 170 Oe and 332 kHz. The samples were dissolved in distilled water and sonicated during 10 min. The temperature of particle suspension is measured with a fiber optical thermometer and registered with data acquisition system. The temperature increase in the samples is measured during 20 min.

The amount of heat generated by magnetic nanoparticles is normally quantified in terms of the SAR, which can be calculated by [13]:

$$\mathrm{SAR} = \frac{\rho C_w}{\mathrm{mNP}}\left(\frac{\Delta T}{\Delta t}\right) \tag{2}$$

where C_w is the specific heat capacity of water (4.185 J/g·k), ρ is the density of the colloid, mNP is the concentration of the magnetic nanoparticles in the suspension and $\Delta T/\Delta t$ is the initial slope of the time-dependent temperature curve. This gives SAR the units W/g [14]. The fundamental problem with this parameter is that SAR is extrinsic and varies depending on both H (field strength) and f (frequency). Therefore, measurements are only comparable if made on the same machine that has the same H and f [15]. We have considered the rise in temperature for the initial 30 s to calculate the slope.

3. Results and Discussions

3.1. Structure, Morphology and Magnetic Properties

The X-ray diffraction patterns for Fe_2O_3 and γ-Fe_2O_3/Gd_2O_3 powders as received and milled for several times are shown in **Figure 1**. Practically, the pat-

terns of as-received γ-Fe_2O_3 powder shows a series of five clear diffraction peaks with the strongest one (311) plane occurring at $2\theta = 35.78^\circ$. The other clear peaks have occurred at $2\theta = 30.52^\circ$, 43.46°, 57.56°, and 63.12° which assigned to (220), (400), (511), and (440) planes respectively. With increasing milling time, the diffraction peaks became broader and their relative intensity decreases. This effect is a typical behavior of materials after milling and attributed usually to the presence of crystallites with small sizes and due to the strain induced by milling. The most dominant crystalline phase is γ-Fe_2O_3 but it is important to notice the presence of two clear peaks due to Gadolinium oxide crystal phases which have occurred at $2\theta = 28.62^\circ$ and 30.32° which corresponding to (222) and (400) planes respectively. For longer milling time, progressive disappearance of some diffraction peak of γ-Fe_2O_3 are observed. For increasing milling time, the shift of peak position towards lower angle (2θ) is observed. An example of this angle shift is highlighted by considering one of characteristic peak corresponding to (311) plane (Figure 1) This shifting of peaks toward the lower angle indicates an increase of lattice parameters with increasing milling time, so, Gd is incorporated with Fe lattice and produced γ-Fe_2O_3/Gd_2O_3 as a nanocomposite.

The crystallite size changes monotonically with the increase of milling time (Table 1). When the milling time is increased from 5 h to 30 h, an increase of crystallite size is observed. This behavior might be due to the agglomeration of crystallite size for longer milling.

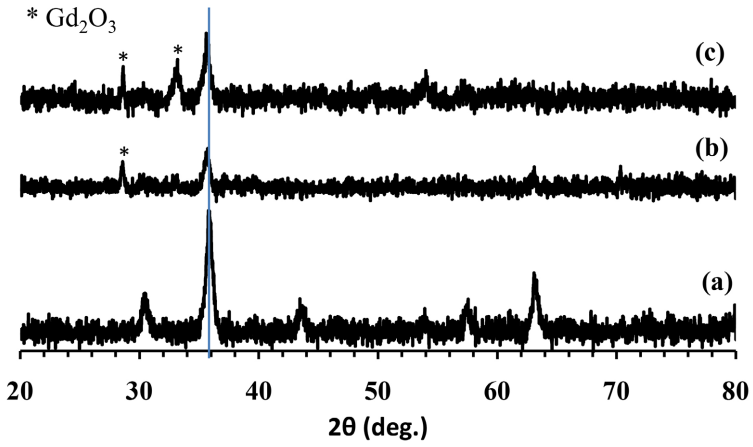

Figure 1. XRD patterns of (a) γ-Fe_2O_3, as received (b) γ-Fe_2O_3/Gd_2O_3 nanostructure for 5 h milling time and (c) γ-Fe_2O_3/Gd_2O_3 nanostructure for 30 h milling time.

Table 1. Average crystallite size of γ-Fe_2O_3 and γ-Fe_2O_3/Gd_2O_3 nanostructures for different milling times.

Sample	Time of milling (h)	D (nm)
γ-Fe_2O_3	0	18
γ-Fe_2O_3/Gd_2O_3	5	38
γ-Fe_2O_3/Gd_2O_3	30	49

The SEM images of the samples milled for 5 h and 30 are depicted in Figure 2. It can be seen that morphology of nanocomposites milled for 5 h shows that the shape is quasi-spherical, the size is in the nanometer scale and the particles are relatively agglomerated (Figure 2(a)). After milling time of 30 h (Figure 2(b)), the particles are agglomerated compared to the sample milled for 5 h.

The vibrating sample magnetometer (VSM) was used to determine the magnetic properties of samples as received and ball milled for different milling times. Figure 3 shows the magnetization-field (M-H) curves recorded at room temperature for the as-received Fe_2O_3 and milled powders. It can be seen that γ-Fe_2O_3 is completely ferromagnetic. It can be seen also that presents hysteresis with small coercivity and remanence. The magnetic parameters deduced from M-H curves are summarized in Table 2.

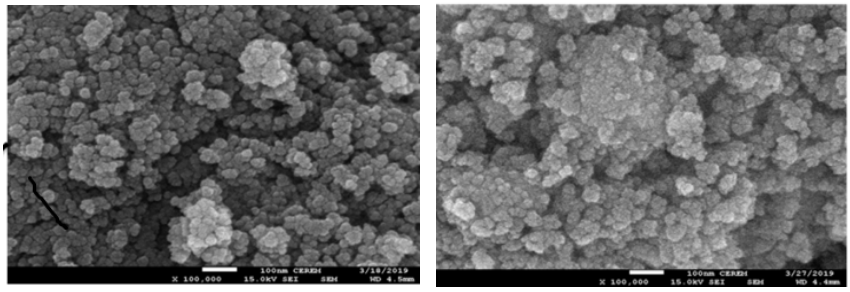

(a) (b)

Figure 2. SEM images of (a) sample milled for 5 h, and (b) milled for 30 h.

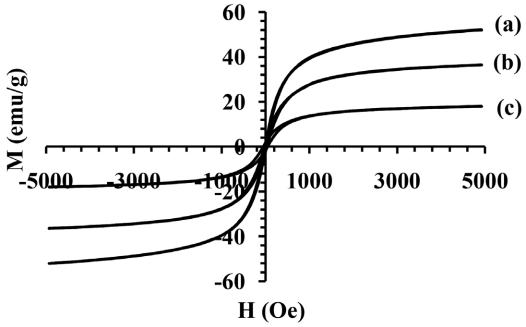

Figure 3. Magnetization (M) versus magnetic field (H) curves of (a) γ-Fe_2O_3, (b) γ-Fe_2O_3/Gd_2O_3 nanostructure for 5 h milling time and (c) γ-Fe_2O_3/Gd_2O_3 nanostructure for 30 h milling time.

Table 2. Ms, Mr and Hc for γ-Fe_2O_3 and γ-Fe_2O_3/Gd_2O_3 nanostructures for different milling times.

Sample	Time of milling (h)	M_s (emu/g)	M_r (emu/g)	H_c (Oe)
γ-Fe_2O_3	0	53	1.4	14
γ-Fe_2O_3/Gd_2O_3	5	37	1.7	27
γ-Fe_2O_3/Gd_2O_3	30	18	2	60

Table 2 indicates the increases of coercivity with increasing milling time, while the saturation decreases. The increase in Hc for the nanocomposite with increasing milling time can be explained by magnetic anisotropy induced by ball milling. Regarding the decreases of the magnetic saturation (Ms), that might be attributed to the site preference of Gd ions. Increasing milling time might affect Fe-Gd interactions and that will affect the magnetic behavior of the nanocomposite. Zhang *et al.* reported similar behavior of Gd doped magnetite nanoparticles [16].

3.2. SAR Measurements

The heating efficiency is studied for the as-prepared nanostructures with concentration of 10 mg/mL at applied field of 170 Oe and frequency of 332 kHz. Figure 3 shows the temperature increase due to the nanocomposite when submitted to an alternating magnetic field. It can be seen from Figure 4 that Fe_2O_3/Gd_2O_3 5 h milling time has best heating compared to that of 30 h milling time. Furthermore, the value of SAR calculated by Equation (2) for 5 h milling time nanocomposite (68 W/g) is higher than that obtained for 30 h milling time nanocomposite (28.7 W/g). 5 h milling time nanocomposite reached 42˚C (hyperthermia temperature) in just 5 min 46 s compared to that of 30 h milling time nanocomposite which reached this temperature in 12 min 22 s.

Comparison of SAR values with similar works showed that both samples show relatively a good heating ability (Table 3). SAR obtained for both samples are

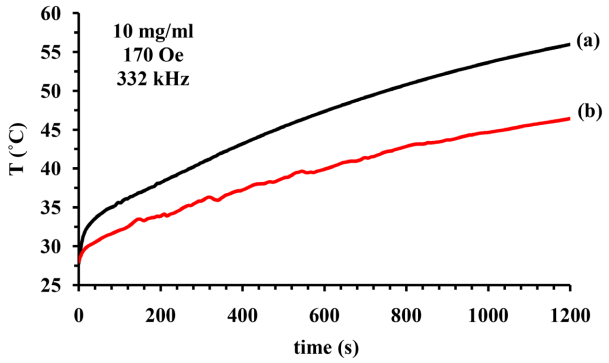

Figure 4. Temperature vs. time of (a) γ-Fe_2O_3/Gd_2O_3 nanostructure for 5 h milling time and (b) γ-Fe_2O_3/Gd_2O_3 nanostructure for 30 h milling time.

Table 3. Comparison of SAR values for different magnetic ferrofluids.

Ferrofluids	Synthesis method	Frequency (kHz)	Field (mT)	SAR (W/g)	References
Gd_2O_3-Fe_2O_3 nanocomposite	Ball milling	332	17	68	This work
Chitosan coated Gd_2O_3-Fe_2O_3	Ball milling	332	17	18.5	[17]
PVP-Fe_3O_4	Hydrothermal	332	17	160	[18]
PAA-Fe_3O_4	Hydrothermal	332	17	36	[19]
Fe_2O_3@TiO_2	Sol-gel	332	17	30	[20]

higher than that reported for ball milled chitosan coated Gd_2O_3-Fe_2O_3 nanocomposite (18.5 W/g) [17]. The heating efficiency is also better than PAA coated magnetite and Fe_2O_3-TiO_2 nancomposite [19] [20].

4. Conclusion

Ball milling technique was used to prepare γ-Fe_2O_3/Gd_2O_3 nanocomposite for possible use in magnetic hyperthermia application. In order to investigate the effect of milling time on this sample, two samples were prepared for different milling time. Milling for longer time induces an increase of the coercivity, a decrease of magnetic saturation, an increase of the crystallite size and a decrease of heating efficiency of nanocomposites. It was also observed that the two samples present hysteresis with small coercivity and remanence. The results obtained in this study show that the obtained nanocomposite for 5 h milling time is a promising candidate for magnetic hyperthermia due to its properties which show high heating efficiency and interesting magnetic behavior.

Conflicts of Interest

The author declares no conflicts of interest regarding the publication of this paper.

References

[1] Ito, A., Fujioka, M., Yoshida, T., Wakamatsu, K., Ito, S., Yamashita, T., Jimbow, K. and Honda, H. (2007) 4-S-Cysteaminylphenol-Loaded Magnetite Cationic Liposomes for Combination Therapy of Hyperthermia with Chemotherapy against Malignant Melanoma. *Cancer Science*, **98**, 424-430. https://doi.org/10.1111/j.1349-7006.2006.00382.x

[2] Gazeau, F., Levy, M. and Wilhelm, C. (2008) Optimizing Magnetic Nanoparticle Design for Nanothermotherapy. *Nanomedicine*, **3**, 831-844. https://doi.org/10.2217/17435889.3.6.831

[3] Jordan, A., Wust, P., Fahling, H., John, W., Hinz, A. and Felix, R. (1993) Inductive Heating of Ferrimagnetic Particles and Magnetic Fluids: Physical Evaluation of Their Potential for Hyperthermia. *International Journal of Hyperthermia*, **9**, 51-68. https://doi.org/10.3109/02656739309061478

[4] Lemine, O.M., Omri, K., El Mir, L., Velasco, V., Crespo, P., De Presa, P., Bouzid, H., Youssif, A. and Hajry, A. (2014) γ-Fe_2O_3 by Sol-Gel with Large Nanoparticles Size for Magnetic Hyperthermia Application. *Journal of Alloys and Compounds*, **607**, 125-131. https://doi.org/10.1016/j.jallcom.2014.04.002

[5] De la Presa, P., Luengo, Y., Multigner, M., Costo, R., Morales, M.P., Rivero, G. and Hernando, A. (2012) Study of Heating Efficiency as a Function of Concentration, Size, and Applied Field in γ-Fe_2O_3 Nanoparticles. *The Journal of Physical Chemistry C*, **116**, 25602-25610. https://doi.org/10.1021/jp310771p

[6] Bohara, R.A., Thorat, N.D., Chaurasi, A.K. and Pawar, S.H. (2015) Cancer Cell Extinction through a Magnetic Fluid Hyperthermia Treatment Produced by Superparamagnetic Co-Zn Ferrite Nanoparticles. *RSC Advances*, **58**, 47225-47234. https://doi.org/10.1039/C5RA04553C

[7] Qiao, D.K., Deng, Y., Ho, C.-C., Ho, C.-Y., Chen, B.-C., Wen, M.-Y. and Xiong,

C.-W. (2023) Effects of Sizes and Anisotropy Constants of Magnetic Nanoparticles on Hyperthermia Temperature Increase with Time. *Science of Advanced Materials*, **13**, 718-723.

[8] Suryanarayana, C. (2001) Mechanical Alloying and Milling. *Materials Science*, **46**, 1-184. https://doi.org/10.1016/S0079-6425(99)00010-9

[9] Lemine, O.M. and Alrub, S.A. (2019) Mechanically Milled $Co_{1-x}Fe_xO_4$ Nanocrystalline for Magnetic Hyperthermia Application. *Journal of Nano Research*, **59**, 25-34. https://doi.org/10.4028/www.scientific.net/JNanoR.59.25

[10] Ban, I., Stergar, J., Drofenik, M., Ferk, G. and Makove, D. (2011) Synthesis of Copper-Nickel Nanoparticles Prepared by Mechanical Milling for Use in Magnetic Hyperthermia. *Journal of Magnetism and Magnetic Materials*, **323**, 2254-2258. https://doi.org/10.1016/j.jmmm.2011.04.004

[11] Langford, J.I. and Wilson, A.J.C. (1978) Scherrer after Sixty Years: A Survey and Some New Results in the Determination of Crystallite Size. *Journal of Applied Crystallography*, **11**, 102-113. https://doi.org/10.1107/S0021889878012844

[12] Uvarov, V. and Popov, I. (2013) Metrological Characterization of X-Ray Diffraction Methods at Different Acquisition Geometries for Determination of Crystallite Size in Nano-Scale Materials. *Materials Characterization*, **85**, 111-123. https://doi.org/10.1016/j.matchar.2013.09.002

[13] Pham, X.N., Nguyen, T.P., Pham, T.N., Tran, T.T.N. and Tran, T.V.T. (2016) Synthesis and Characterization of Chitosan-Coated Magnetite Nanoparticles and Their Application in Curcumin Drug Delivery. *Advances in Natural Sciences*: *Nanoscience and Nanotechnology*, **7**, Article ID: 045010. https://doi.org/10.1088/2043-6262/7/4/045010

[14] Babincova, M., Leszczynska, D., Sourivong, P., Cicmanec, P. and Babinec, P. (2001) Superparamagnetic Gel as a Novel Material for Electromagnetically Induced Hyperthermia. *Journal of Magnetism and Magnetic Materials*, **225**, 109-112. https://doi.org/10.1016/S0304-8853(00)01237-3

[15] Kallumadil, M., Tada, M., Nakagawa, T., Abe, M., Southern, P. and Pankhurst, Q.A. (2009) Suitability of Commercial Colloids for Magnetic Hyperthermia. *Journal of Magnetism and Magnetic Materials*, **321**, 1509-1513. https://doi.org/10.1016/j.jmmm.2009.02.075

[16] Zhang, H.H., Malik, V., Mallapragad, S. and Akinc, M. (2017) Synthesis and Characterization of Gd-Doped Magnetite Nanoparticles. *Journal of Magnetism and Magnetic Materials*, **423**, 386-394. https://doi.org/10.1016/j.jmmm.2016.10.005

[17] Lemine, O.M., Alanazi, A., *et al.* (2020) γ-Fe_2O_3/Gd_2O_3-Chitosan Magnetic Nanocomposite for Hyperthermia Application: Structural, Magnetic, Heating Efficiency and Cytotoxicity Studies. *Applied Physics A*, **126**, Article No. 471. https://doi.org/10.1007/s00339-020-03649-5

[18] El-Boubbou, K., Lemine, O.M., Ali, R., Huwaizi, S.M., Al-Humaid, S. and AlKushi, A. (2022) Evaluating Magnetic and Thermal Effects of Various Polymerylated Magnetic Iron Oxide Nanoparticles for Combined Chemo-Hyperthermia. *New Journal of Chemistry*, **46**, 5489-5504. https://doi.org/10.1039/D1NJ05791J

[19] Algessair, S., Lemine, O.M., Madkhali, N., *et al.* (2023) Tuning the Heat Dissipated by Polyacrylic Acid (PAA)-Coated Magnetite Nanoparticles under Alternating Magnetic Field for Hyperthermia Applications. *Applied Physics A*, **129**, Article No. 814. https://doi.org/10.1007/s00339-023-07097-9

[20] Lemine, O.M., Madkhali, N., Alshammari, M., Algessair, S., Gismelseed, A., El Mir, L., Hjiri, M., Yousif, A.A. and El-Boubbou, K. (2021) Maghemite (γ-Fe_2O_3) and

γ-Fe_2O_3-TiO_2 Nanoparticles for Magnetic Hyperthermia Applications: Synthesis, Characterization and Heating Efficiency, *Materials*, **14**, Article No. 5691. https://doi.org/10.3390/ma14195691